Osteoporosis Screening: Applied Methods and Technological Trends

Mario A. de Oliveira [*,a], Raimes Moraes [b], Everton B. Castanha [c], Alexandra S. Prevedello [d],
Jozue Vieira Filho [e], Frederico A. Bussolaro [d], David García Cava [f]

[a] *School of Engineering and the Built Environment, Birmingham City University, Birmingham, B47XG, United Kingdom*
[b] *Department of Electrical and Electronic Engineering, Federal University of Santa Catarina, Florianopolis, 88040-900, Brazil*
[c] *Faculty of Medicine, Federal University of Pelotas, Pelotas, 96030-000, Brazil*
[d] *Health Science Institute, Federal University of Mato Grosso, Sinop, 78550-728, Brazil*
[e] *Telecommunications and Aeronautical Engineering, São Paulo State University (UNESP), So Jḻao da BoaVista, 13876-750, Brazil*
[f] *School of Engineering, The Institute for Infrastructure and Environment, The University of Edinburgh, Edinburgh, EH93FG, United Kingdom*

ABSTRACT

Bones are continuously remodeled (resorbed and regenerated) to allow fracture healing and skeleton adaptation to stress. When excessive resorption occurs, bone microstructure is deteriorated, leading to osteoporosis. At early stages, osteoporosis usually has no symptoms; most people are diagnosed when a fracture occurs due to disease severity. To prevent fractures, technologies have been developed to identify high risk population eligible to treatment. Fracture risk has been assessed by analyzing the interaction of different energy stimulus with bone tissues as well as by statistical models that evaluate multiple clinical risk factors. The most applied methods are Dual-energy X-ray Absorptiometry and Fracture Risk Assessment tool. As they present some limitations, other technologies have been proposed for such purpose. A survey of the currently applied and emerging methods is here presented in order to provide a scenario of the technological challenges and trends to diagnose osteoporosis.

1. Introduction

Osteoporosis affects 200 million women [1]. For the population over 50 years old, it is estimated that the percentages of men and women with osteoporosis are, respectively: 16.0% and 29.9% in the USA [2], 6.8% and 22.5% in European Union [3], 6% and 23% in Australia [3], 6.46% and 29.13% in China [4]. In Latin America, estimates of hip fractures for women and men aged from 50 to 64 years old indicate an increase of 400% between 1990 and 2050; a growth around 700% for the population over 65 years old [1]. In Brazil, over 10 million people have osteoporosis (one in 17 people); however, only a third of patients with osteoporotic hip fracture is diagnosed and a fifth of such patients receives treatment [5,6].

In six European nations (France, Germany, Italy, Spain, Sweden, and the UK), 2.7 million osteoporotic fractures occur every year with an associated healthcare expenses of US$40.7 billion; it is expected a 23% cost increase by 2030 (US$ 51.7 billion) [7]. Among Medicare beneficiaries (American Healthcare Trust Fund), there were 2.3 million osteoporotic fractures in 2015; costs of US$57 billion were estimated in 2018 with an expected increase over US$95.2 billion in 2040. Such estimates take into account the population aging and growth [8].

Bones provide structural support for locomotion, protection of internal organs, calcium and phosphate storage, as well as produce hormones to regulate mineral and energy metabolism [9]. Total bone mass is composed of, approximately, 80% of cortical tissue and 20% of trabecular tissue, but their proportion varies in each bone, establishing the bone's strength. For example, long bones have more cortical tissue and vertebrae contain more trabecular one [10]. Trabecular bone is less dense and more flexible and fragile than cortical bone, presenting higher metabolic activity [11].

During their life cycles, bones are continuously renewed through a remodeling process (composed of two phases resorption and regeneration) for skeleton adaptation to mechanical stress as well as for fracture healing. Bone resorption without proper reposition by specialized cells reduces mass and causes micro architectural deterioration of the tissue. When a clinically significant imbalance occurs, the individual is diagnosed with osteoporosis; that is, a systemic skeletal disease that causes bone fragility and susceptibility to fracture [12]. Osteopenia is also associated to reduced bone mineral content, being less severe than osteoporosis. After the age of 20, bone resorption becomes predominant
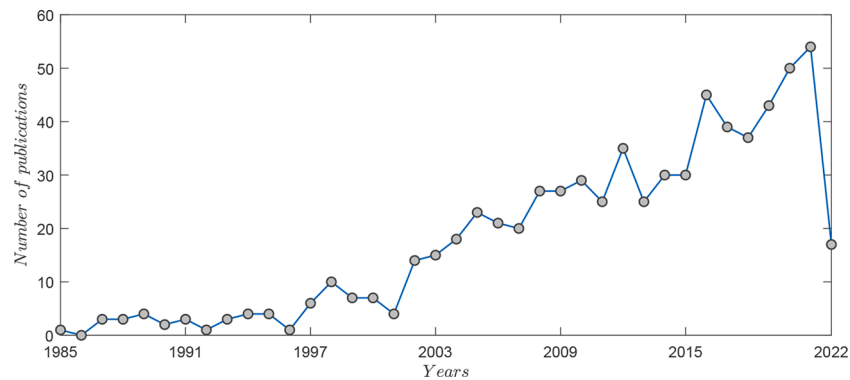
Fig. 1. Number of publications in the field of osteoporosis screening methods in the period between 1985 and 2022 (www.scopus.com, consulted 05/05/2022) (Keywords: Osteoporosis + screening).

in men and its mineral content declines about 4% per decade. Females generally maintain the peak mineral content until menopause; thereafter, it declines about 15% per decade [13], first affecting the trabecular bone [12]. Osteoporosis affects to all old individuals [14]. Above a third of older women and a quarter of older men have fractures related to fragile bones [8]. Some people have osteoporosis at an earlier life stage due to illness, medication or hormonal deficiency [15]. Frequent intake of glucocorticoids (recommended for inflammatory rheumatic diseases and lung disorders) doubles the risk of fractures in both sexes [16]. Other risk factors are: smoking, alcoholism, physical inactivity, and improper diet. Based on the etiology, osteoporosis is classified as primary (due to genetic illnesses and aging) or secondary (caused, for example, by immunosuppressive drugs).

Osteoporosis has no symptoms and most people are diagnosed when fracture occurs due to disease severity [17,18]. Such fractures lead to chronic health problems. Its global impact is increasing due to population aging, demanding worldwide efforts to prevent bone fractures [11, 19,20]. Screening to find out high risk population eligible to treatment (among others, administration of calcium and vitamin D) may reduce social and economic burden.

A common diagnostic test for osteoporosis is bone densitometry. Dual-energy X-ray absorptiometry (DXA) is pointed out by the World Health Organization (WHO) as the gold standard to measure bone mineral density [13]. Based on such measurement, diagnosis of osteoporosis and the assessment of fracture risk has been carried out. However, WHO also suggests the investigation of alternative technologies for such purpose [21]. Currently, there is no accepted policy to identify patients with high risk of fracture in Europe [22]. Thus, there is a clear need for technology development to complement the existing procedures for osteoporosis diagnosis, aiming to improve the results as well as to reduce the associated technological costs in order to allow an

universal coverage.

Unlike other reviews, this survey does not only focus on current methods to assist the osteoporosis diagnosis, but also discusses technologies that have been investigated to enhance osteoporosis management and reduce exam costs. Thus, the reader has a scenario of current trends and efforts to develop technologies to characterize bone health.

The remainder of this text is structured as follows. Section 2 describes the literature review (database, search terms, inclusion and exclusion criteria). Section 3 presents the current technologies available in the market to assist osteoporosis diagnosis. Section 4 reports new approaches that have been been investigated for this purpose. Section 5 discusses the current scenario and concludes this review.

2. Search Methodology

There is a vast literature on osteoporosis screening methods; thus, it was necessary to limit the search scope. Using the words "osteoporosis + screening", search in the Scopus database (title, abstract and keywords) resulted in 687 records from 1985 to 2022 (Fig 1). As observed in Fig 1, there was significant increase of publications in the last 20 years. It shows that the population aging has raised concerns about the impact of osteoporosis on public health.

Search for the words "osteoporosis + review" found out 33 records published between 1968 and 2022 (Fig 2). Most reviews discuss medical perspectives on treatments, clinical diagnosis, prevention, and cost-effectiveness. Search for the words "osteoporosis + technologies" had only three findings [23–25]. During our searches, a paper was found that discusses current applied technologies without presenting new technologies being investigated for such purpose as carried out in this review [26].

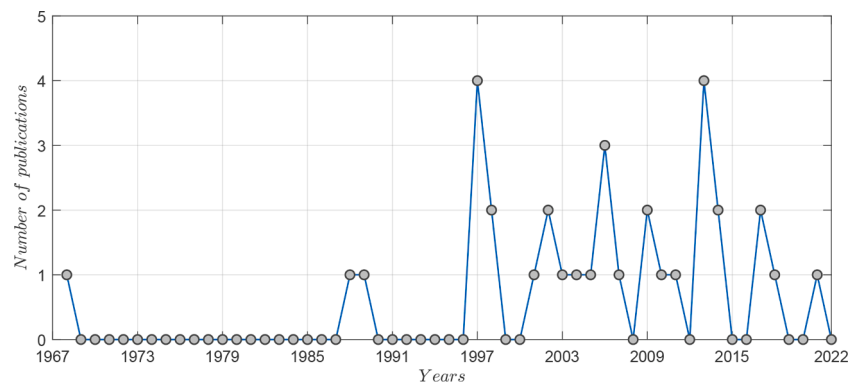We could not find any manuscript that surveys current and emerging

Fig. 2. Number of publications in the field of osteoporosis review methods in the period between 1968 and 2022 (www.scopus.com, consulted 05/05/2022) (Keywords: Osteoporosis + review).
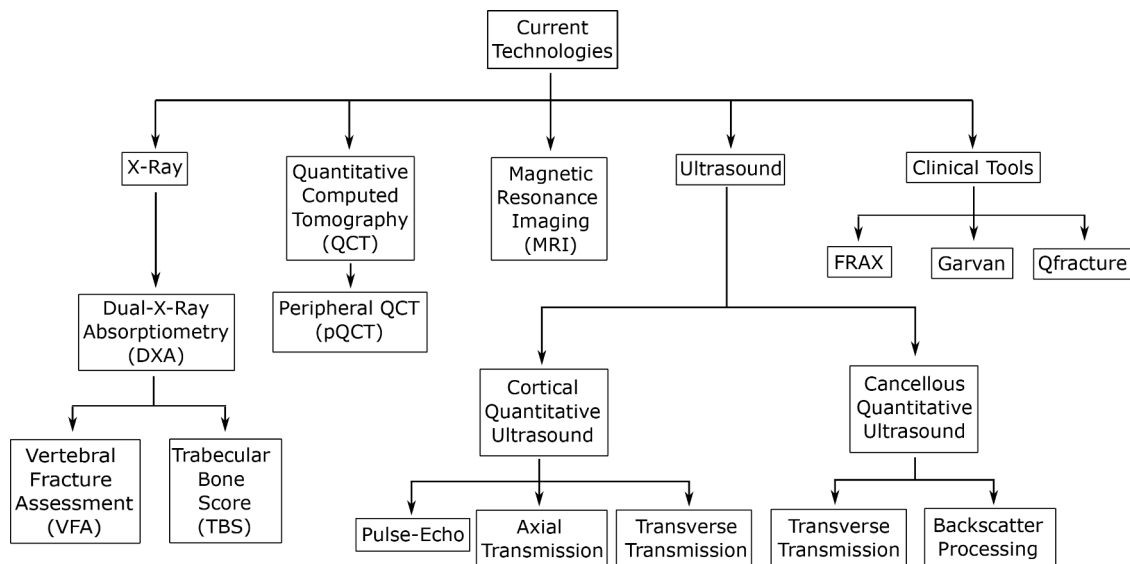
Fig. 3. Scheme of the current technologies for osteoporosis diagnosis.

technologies applied to diagnosis of osteoporosis, aiming to provide a wide view of the technological challenges in this field. Hence, this review summarizes the working principles of different technologies for osteoporosis diagnosis, highlighting their advantages and limitations.

3. Current Applied Technologies

Currently, there exist several commercial devices and computer tools to assist osteoporosis diagnosis. However, all of them have limitations, as pointed out in the following subsections, demanding additional developments to circumvent them. This section is presented according to the structure of Fig 3.

3.1. Dual-energy X-ray Absorptiometry

DXA is considered the gold standard for measuring bone mineral density (BMD), since it has been intensively investigated and validated worldwide. DXA systems generate X-ray beams with two different levels of energy. The absorption of the high (e.g. 71 keV) and low (e.g. 39 keV) energy beams by the different body tissues allows the quantification of BMD. Bone minerals (e.g. calcium) absorb more low energy X-rays beams than soft tissues. The attenuation imposed by soft tissues to the X-ray beams in body regions without bones is used as a baseline measurement. Bone mineral content is then estimated by subtracting attenuation ratio between low and high energy X-rays through tissue and bone from the baseline measurement. The system also does a X-ray sweep on the region of interest in order to provide images. There are differences among DXA systems of different manufacturers regarding to X-ray beams generation, energy range, X-ray detectors, and body sweeping method [27].

BMD (g/cm^2) is given by the ratio between the measured bone mineral content (grams) and the measured area of the bone (cm^2). For diagnosis purpose, bone density values are usually reported as standard deviation units related to the normal probability density distribution of a uniform Caucasian female control group [28], the T-score:

$$\text{T-score} = \frac{S_{BMD} - \mu_C}{\sigma_C} \tag{1}$$

where S_{BMD} is a new BMD measurement, μ_C and σ_C are the mean and the standard deviation of the normal distribution, respectively. The reference values for normal subjects, low bone density (osteopenia), and osteoporosis are respectively: T-score $\geq$ -1, -1 > T-score > -2.5, T-score $\leq$ -2.5 [21].

BMD should be measured from posterior-anterior spine (L1 to L4, excluding the ones with structural damage) and hip (lowest BMD value between proximal femur or femoral neck). In case of hyperparathyroidism or obesity, BMD may be measured from forearm (1/3 distal radius).

BMD measurements in children, who have not achieved their peak bone mass, is carried out by means of the Z-score. Z-score can be calculated similarly to Eq. 1, replacing the control group values (mean and standard deviation) for those of a matched population taking into account the same age range, gender, and ethnicity. Z-score is also recommended for prior menopausal women and men under 50 years. A Z-score of -2.0 or lower is defined as "below the expected range for age" and a Z-score above -2.0 is "within the expected range for age" [21].

Despite being largely used, the analyzes of DXA measurements demand attention. Since BMD is based on X-rays attenuation, lumbar vertebra compressed by a fragility fracture may generate measurement artifact; a high BMD value may be related to an increased vertebra thickness instead of high mineral content. To circumvent that, if a BMD measurement obtained for given vertebra is very large when compared to the others, it shall be excluded from the calculated indices.

As mentioned, T-score is calculated using a control group as reference. Ideally, there should be available an ethnically-defined reference database for each examined subject. That is particularly difficult to manage in nations with large racial diversity [29].

Different manufacturers do not use a common database or a same technology to generate their measurements. Therefore, follow-up of patients should be conducted in the same facility, same bone region, and same device [19]; even though, database or device software may be updated. Thus, BMD is more suitable for patient monitoring instead of T or Z-scores. Besides, operators should be trained as correct patient positioning should be observed [29]. Quality control procedures should be weekly followed to assure repeatability of DXA measurements. Such aspects hamper the follow-up of patients' treatment.

The American College of Physicians points out that there are no evidences to recommend DXA monitoring for patients with normal BMD, neither during the initial five years of pharmacological treatment of osteoporosis [30]. Besides, the cost of DXA devices is high, generally over US $35,000. Thus, further development of currently investigated technologies may provide more powerful tools to improve osteoporosis screening.

Quantitative indices of hip geometry calculated from DXA images have been investigated to assess fracture risk [31,32]. Researchers have

proposed a statistical model based on joint BMD and femur shape measurements to improve hip fracture risk assessment when compared to that carried out by only T-score [33]. Currently, only proximal hip axis length (HAL) index (distance from the inner pelvic brim to the greater trochanter) is recommended to assess hip fracture risk of post-menopausal women [28].

It has been pointed out that quantitative indices obtained by DXA overlook localized bone weakness, hampering the diagnosis. Complementary techniques have been proposed to improve the patient's evaluation such as vertebral fracture assessment and trabecular bone score.

3.1.1. Vertebral Fracture Assessment

Lateral spine images for vertebral fracture assessment (VFA) may be acquired by DXA when measuring BMD. Such method allows a radiation dose 200 times lower than that of standard X-ray devices, being less expensive [34]. DXA images of vertebrae superior to T7 have inferior quality when compared to those of standard radiographs, but their fracture is relatively uncommon in older women [35].

Fractures have been identified by lateral spine images in patients with and without osteoporosis according to the BMD criteria; such findings influence the prescription of preventive medication to avoid new vertebral and non-vertebral fractures [36].

The International Society for Clinical Densitometry (ISCD) recommends VFA when T-score is inferior to -1 associated to one (or more) of the following conditions: women above 70 years, men above 80 years, height loss superior to 4 cm, previous vertebral fracture, glucocorticoid therapy for three months [34]. The United Kingdom National Osteoporosis Guidelines Group (UK NOGG) recommends VFA for postmenopausal women as well as for men age 50 years and older who have height loss equal or greater than 4 cm, kyphosis, recent or current long-term oral glucocorticoid therapy, or a BMD T-score $\leq$ -2.5 at either the spine or hip, or in cases of acute onset back pain with risk factors for osteoporosis [37].

3.1.2. Trabecular Bone Score

Bone resistance to fractures is determined by many factors, such its micro and macro structures, BMD, and adjacent tissues (e.g., cartilages, muscles). Such complementary factors shall be analyzed when BMD alone does not explain increased fracture risk (e.g., presence of desmophytes in vertebral column) [38,39].

Trabecular bone score (TBS), obtained from DXA images, indirectly assesses the trabecular microstructure. A heterogeneous bone density causes irregular photon absorption that can be detected by grey level changes among pixels belonging to two-dimensional (2D) lumbar spine DXA images. The so-called variogram is the sum of the squared grey level differences between pixels at a specific distance. TBS is calculated as the slope of the log-log transform of the 2D variogram to characterize the rate of grey level amplitude variations. A high TBS value is related to fracture-resistant bone [39].

Since DXA image resolution (0.5 mm) is not enough to solve bone microstructure, TBS is actually related to macroscopic vertebrae features resulting from microarchitectural arrangements. TBS is affected by soft tissue composition and thickness. Such factors may be compensated by software adjustments that take into account body mass index (BMI). As TBS comes from DXA images, its measurements depend on proprietary manufacturers' technologies [40,41].

Recent work did not find relation between TBS and a vertebral fracture severity index based on VFA; the authors suggested the use of both indices to characterize bone strength [42]. A similar result was found when comparing TBS to quantitative ultrasound (QUS), suggesting that both techniques assess different characteristics of bones [43].

TBS has been pointed out as an useful index to assist the osteoporotic fracture risk assessment of postmenopausal women and men older than 50 years [44–46]. It may be also useful to assess patients with osteophytes, since such condition leads to inaccurate BMD measurements [47,48]. However, it shall not be used for patients' follow-up, since its value

is not proportional to BMD increasing [41,49]. Additional research is recommended to better establish its applicability [50–52].

3.2. Quantitative Computed Tomography

Computed tomography (CT) generates cross-sectional images after processing multiple X-ray planes acquired at different body angles. For that, X-ray beam and detectors are rotated around the patient during the exam [53,54]. Thus, a CT scan is assembled based on a set of images (usually contiguous) obtained from the area of interest. The grey-scale of CT images is associated to the relative attenuation imposed by the interrogated structures, being estimated for each region of the cross-sectional image.

Quantitative computed tomography (QCT) allows the analysis of CT images beyond a visual radiological evaluation. Quantitative parameters are measured from structures and texture of bone images [55–57]; for instance, vertebral strength has been estimated by finite element analysis of QCT scans [58].

QCT is generally obtained from lumbar spine and hip by means of standard whole-body CT scanners and dedicated software. Other bones investigated by QCT are proximal femur, forearm, and tibia [56,59].

QCT plays an import role in the osteoporosis diagnosis since it provides selective trabecular BMD measurement (tissue more affected by metabolic diseases) and has superior soft tissue differentiation [60].

Since DXA is used as gold standard, its comparison to CT has been recently carried out [56,61,62]. For instance, fracture risk indices estimated from DXA-based (two-dimensional) and CT-based (three-dimensional) finite-element models have shown significant correlation [63]. However, CT provides a better sensitivity and more accurate data [26,59,63].

In contrast to DXA, all CT scanners are similarly calibrated [55]. QCT is less susceptible to confounding factors such as superimposition of overlying structures, spinal degenerative changes, aortic calcification, bone size, and BMI [61]. Thus, femoral neck and total hip T-scores calculated from two-dimensional projections of QCT data are considered equivalent to DXA T-scores for diagnosis of osteoporosis [27]. However, movement artifacts during QCT scanning can lead to misinterpretations [53].

QCT is a complex procedure with low availability, high cost, and relative high radiation exposure [26,55,59]. To circumvent these two last aspects, researchers propose opportunistic screening when CT scans obtained to assess other health conditions (acquired from chest, abdomen, pelvis, and spine) are used to diagnose osteoporosis. [61,64,65].

Multivariate linear regression analysis (MLRA) has been successfully applied to QCT, assisting the evaluation of osteoporosis in subjects with normal glucose tolerance, impaired glucose tolerance, and diabetes [66].

A deep learning model was used to analyse processed images of upper lumbar vertebrae obtained by means of low dose chest CT, ordinarily used for early lung cancer diagnosis. The proposed system had good performance to automatically detect osteoporosis and low BMD [61].

Recently, hip fracture risk prediction was assessed by means of a partial least square based statistical model of the proximal femur taking into account three-dimensional bone geometry measurements and BMD distribution obtained by CT. Results of the proposed model applied to a sample group of 100 Caucasian women show that it substantially enhances fracture risk prediction when compared to areal BMD measured by DXA [67].

In a clinical study with 98 prostate cancer patients using a combination of FRAX (Section 3.5) and mean attenuation of the mid-L5 vertebra measured from pelvic CT, the assessment of hip fracture risk was not significantly improved [68]. Among other factors, the results were associated to the small number of only male subjects.

CT-based and FRAX without BMD (FRAXwb) predictors were

investigated to improve the detection of high fracture risk individuals [65]. A CT-based prediction tool based on linear regression was developed, using as input three bone imaging biomarkers along with age and sex data; contribution of FRAXwb to the CT-based prediction tool was also assessed. The authors concluded that when FRAXwb input is not available, the initial evaluation of fracture risk can be carried out automatically based on a single abdomen or chest CT.

Biomechanical computed tomography (BCT) has been proposed to identify high fracture risk patients based on both femoral strength and hip BMD T-scores [69]. The clinical outcomes were obtained using a four states Markov model along a year, which includes: presence and absence of hip fractures, osteoporosis treatment, and bone's death (absorbing state). BCT also comprises a virtual stress test, advanced medical image processing, bone biomechanics concepts, and non-linear finite element analysis to predict typical fracture [70].

Cone beam computed tomography (CBCT), used in oral and maxillofacial surgery, has been investigated as a screening tool for early detection of osteoporosis and subsequent referral [71]. As advantage, CBCT offers lower radiation exposure than QCT. In [72], the diagnosis of osteoporosis is proposed for postmenopausal women with normal BMD by using a composite osteoporosis index (three-dimensional mandibular osteoporosis index: 3D MOI) measured by CBCT. 3D MOI showed good performance to assess, qualitatively and quantitatively, osteoporosis in the mandibular cortex.

3.2.1. Peripheral Quantitative Computed Tomography

Peripheral QCT (pQCT) consists of the application of QCT to appendicular skeleton sites, such as arms or legs. Compared to general CT scanners, pQCT devices have similar data acquisition and reconstruction procedures, but have higher mobility, employ less radiation, and have lower cost [55,73].

High-resolution pQCT (HR-pQCT) allows a much more detailed follow up of patients under treatment compared to DXA [74,75]. HR-pQCT has also been successfully applied to analyze subchondral trabecular bone in patients with medial knee osteoarthritis [76]. Assessment of trabecular bone architecture and BMD at the distal radius and tibia by HR-pQCT has shown reproducibility and ability to detect aging and disease-related changes [77].

Lately, finite element (FE) models and pQCT have also been successfully applied to compute bone strength and stiffness of forearm (i.e. distal radius) [78]. It was observed that FE modelling allows the assessment of osteoporotic bone strength. FE modelling was also employed to identify patients with peripheral low-trauma fracture. Therefore, pQCT-FE enhanced the diagnosis when compared to standard pQCT and DXA [79].

3.3. Magnetic Resonance Imaging

Magnetic resonance imaging (MRI) is often used for visualization of human organs due to its inherent soft tissue contrast. For that, static and transient magnetic fields are applied to the body. Excited hydrogen atoms of the interrogated tissues (contained, mainly, in water and fat) emit radio frequency (RF) signals while returning to their equilibrium state. The RF signals are sampled by the device receiving coils; their processing allows the characterization of tissues from different body layers.

Bone structure and texture attributes have been obtained from MRI images to characterize vertebral fragility or fracture. For that, MRI images are usually pre-processed and segmented, before having the features extracted and classified. Further development of these methods may provide tools for opportunistic screening of osteoporosis [80,81].

As trabecular marrow contains water and fat, MRI systems (1.5, 3, and 7 Tesla) have been applied to characterize trabecular microarchitecture [82,83]. The investigations have been carried out for small populations ($n<100$, being n the number of patients). Results of comparative analyses point out that the MRI may allow identification of

patients with fracture risk not detected by DXA [82]. Relaxation times and rates (inherent to MRI technology) are also used to investigate trabecular structure and bone density [84].

Visualization of cortical bones requires MRI system with advanced feature (ultra-short echo time) to acquire RF signals from water belonging to cortical microscopic pores and matrix collagen. Quantitative indices to characterize the cortical strength have also been proposed [82].

Advances of MRI technology allowed the inclusion of magnetic resonance spectroscopy (MRS) on the investigation of organs metabolism [85]. As the name suggest, MRS assesses the frequency content of the received RF signals to characterize the composition of bone marrow; its composition may be related to osteoporosis pathophysiology. As different devices use different software to analyze MRS data, researchers may have large variability among their results [85,86].

MRI does not involve ionizing radiation, but it is an expensive and a time consuming exam. Techniques for its application to characterize bones are being further developed.

3.4. Quantitative Ultrasound

Methods based on ultrasound have been intensively investigated to provide an alternative to DXA. They aim to be non-invasive, portable, safer (ionizing radiation free), and less expensive technology.

However, quantitative ultrasound (QUS) systems present drawbacks similar to those of DXA. The manufacturers apply different technologies to carry out measurements; thus, different devices provide different quantitative values for a same subject from different skeletal sites [87]. Technologists properly trained shall follow quality control protocols to calibrate the devices. Operator may have impact on the reproducibility of measurements performed by a same device. Due to such aspects, the International Society for Clinical Densitometry (ISCD) recognizes the potential of heel QUS to assess fracture risk, pointing out that it is not effective for monitoring treatment efficacy [88].

3.4.1. Cortical Quantitative Ultrasound

The cortical bone is a dense tissue that surrounds the trabecular one in order to increase the overall mechanical strength of each skeletal component; even though, it has a porous network. Its external surface is named periosteum and its interface with the internal trabecular tissue, endosteum. With aging, the cortical tissue becomes thinner and more porous [89]. Several ultrasound technologies have been proposed to estimate the cortical thickness in order to assist screening and osteoporosis diagnosis.

Pulse-echo Method An ultrasound burst (3 MHz) is applied by means of a focused transducer to interrogate the bone (radius or tibia). Two reflected pulses are received by the same transducer from the periosteum and endosteum interfaces due to acoustic impedance mismatches. The envelopes of the two received bursts are calculated by applying the Hilbert transform. The time interval between their peaks is multiplied by the speed of sound to estimate the cortical layer thickness (Ct.Th). Anthropometric data and Ct.Th measured from different sites (distal radius, proximal and distal tibia) are used to calculate an index named density index (DI). Studies carried out for relative small groups of Caucasian women ($n<1000$) have shown that DI may assist the screening of patients with osteoporosis [90,91].

Further developments of the technology may provide a low-cost device for osteoporosis diagnosis. Despite being commercially available, their clinical application has not been validated yet by means of studies in large multi-racial populations.

Axial Transmission The outer cortical shell of bones is often modelled as a transverse isotropic free plate [92], since it has different acoustic properties from the surrounding soft tissue and internal trabecular tissue. Other models have also been investigated [93,94], but the plate model matches reasonably well to the acoustic transmission observed in experimental setups [95].

In the free plate model, an incident ultrasound pulse causes the propagation of longitudinal and shear waves that interact to generate, as result (depending on the cortical layer thickness and ultrasound frequency), multiple resonant vibration modes known as Lamb waves. They are symmetric and anti-symmetric waves (having the longitudinal axis as reference) that propagate independently of each other.

In axial transmission, an ultrasound probe containing an array of transducers (transmitters and receivers) is placed on the interrogated bone (usually radius or tibia). A transmitted pulse (200 kHz to 1 MHz) is sampled by each receiver (placed at different distances from the transmitter). Owing to the complex Lamb waves propagation, each receiver samples signals that have different waveforms. The array of sampled waveforms (distance vs time) is processed to obtain a two-dimensional (2D) spatio-temporal Fourier transform. From the 2D Fourier transform, the phase velocity of each guided wave mode can be obtained as they correspond to the temporal evolution of local spectral peaks. Theoretical modes computed for the free plate model are fitted to such experimental measurements. As the theoretical model is based on physical parameters (such as Young's modulus), bone properties can be estimated; that is called model-based inversion method.

The initial studies on axial transmission of acoustic waves in bones observed a first arriving signal (FAS) as part of the received ultrasound burst. With the posterior application of Lamb's theory, FAS was associated to the fundamental symmetric Lamb wave [60] for applied acoustic wavelengths comparable or greater than the cortical thickness; such acoustic waves have a larger penetration depth, interrogating deeper bone layers. The FAS velocity (vFAS) has been obtained by measuring the delay between the instant of application and the initial reception time of the ultrasound pulse; knowing the distance between the transducers (transmitter and receivers), the propagation velocity (vFAS) is calculated.

Based on vFAS and phase velocity of other Lamb modes, characteristics (porosity and thickness) of the cortical bone have been investigated. *Ex vivo* and *in vivo* studies have been carried out to compare the estimated cortical properties to those measured by computed tomography [75,96–98]. Future investigations shall allow the improvement of current QUS devices that apply such method.

Meanwhile, axial velocity of ultrasonic waves was employed to assess antiresorptive therapies in a small population (n = 468); it was observed an increase of the velocity measured from tibia over five years when compared to a control group [99].

Velocity of ultrasonic waves along the axial direction has also been investigated at relative high-frequency (3 MHz) to assess the bone microstructure. The purpose is to associate bone anisotropy to the measured velocity in order to assess the tissue integrity [100].

A different approach used a hydrophone to sample, at four different axial distances, acoustic pulses applied to the tibia by an ultrasound probe; based on arrival time measurements of waves propagated to two nearby distances, a median velocity was obtained. For a small *in vivo* sample (n = 27), such median propagation velocity was successfully used to identify three sets of subjects: healthy (n = 13), osteopenic (n = 8), and osteoporotic (n = 6). In this work [101], the authors also modeled the waveform received by the hydrophone as consisting of superimposed multiple echoes from bone (different vibration modes) and soft tissues (interfering signals). To identify the different contributions, the received signal was decomposed in five modes by means of Variational Mode Decomposition (VMD) [102]. Measurements of the median velocity for the mode with maximum power (obtained by VMD) presented better performance than the direct velocity estimation to detect osteoporotic bone.

Transverse Transmission Commercial ultrasound systems also carry out measurements from hand's phalanges. Usually, they measure the time taken by an ultrasound pulse to travel across the distance between two aligned transducers placed on opposite sides of the distal metaphysis; it corresponds to the interval between the pulse application time and the instant when the received signal first achieves the amplitude of 2 mV. The so-called amplitude-dependent speed of sound (AD-SoS) is obtained by dividing such time interval by the distance between the transducers [103]. The mean AD-SoS measured from phalanges of the non-dominant hand has been correlated to BMD measured by DXA [104]. AD-SoS measurements have also been associated to age-related changes in bone mass during pubertal years [105].

3.4.2. Cancellous Quantitative Ultrasound

There are many commercial devices that carry out different quantitative measurements from the heel. 90% of the calcaneus (heel bone) consists of trabecular bone tissue where initial loss of bone mass occurs. The heel can be easily handled; besides, it is not surrounded by a large amount of soft tissue that could hamper the analysis of the results.

Transverse Transmission The velocity and attenuation of ultrasound waves propagating across different materials depend on their physical properties. Velocity depends on the Young's modulus and density; attenuation is related to acoustic impedance, scattering, and absorption. Thus, velocity and attenuation measurements of acoustic waves are associated to characteristics of the interrogated tissue.

To assess the calcaneus, QUS systems usually measure the speed of sound (SoS) and broadband ultrasonic attenuation (BUA). These indices have shown good performance to predict fractures risk [106].

For that, a piezoelectric transducer is used to apply a short duration acoustic wave that, after travelling across the heel, is received by a second transducer (aligned at a fixed or adjustable distance). For acoustic impedance matching, the transducers may be coupled to the heel by means of gel or water; it depends on the system manufacturer. Reference measurements from degassed water are obtained for the ultrasound system. The time interval for the applied pulse to reach the receiver is measured using only water (reference), and later, with the placement of the patient's heel; the difference between these measurements allows the estimation of SoS (m/cm^2) [107]. Technical approaches to carry out such measurement were reviewed [108].

BUA measurement is more complex, since attenuation depends on the ultrasound frequency. As a short acoustic pulse has a broad range of frequencies, discrete Fourier transform is applied to the sampled received signal in order to obtain the amplitude of each frequency component. Attenuation measurements are carried out for frequencies ranging from 300 to 700kHz [108]. Within such range, attenuation is higher for increasing frequencies (linear trend). Thus, it is possible to fit a straight line to the experimental data set (attenuation vs frequency). The angular coefficient of the fitted line is the BUA (dB/MHz). Such index divided by the heel thickness ($dB \cdot MHz^{-1} \cdot cm^{-1}$) is named normalized BUA (nBUA); it allows the comparative analysis of measurements carried out from different subjects.

The propagation of acoustic waves through bone is quite complex since its tissue is anisotropic and inhomogeneous. Several models have been proposed and several experiments have been carried out to better understand it [109].

Among these models, Biot's theory describes longitudinal waves that travel at different velocities (fast and slow) in fluid-saturated porous media, such as the trabecular bone. Fast transmission occurs when solid (trabecular structure) and fluid (bone marrow) move in phase; slow transmission corresponds to solid and fluid moving out of phase during the wave propagation [110]. Experimental results characterized their different interactions with bone tissue. For higher bone densities, propagation velocity of the fast wave increases (2200 to 2700 m/s), being almost constant for the slow wave (about 1400 m/s). Such velocity is almost independent of the applied ultrasound frequency for a range between 0.5 and 5 MHz. The attenuation constant of the slow wave increases with bone density; for the fast wave, the attenuation constant is much higher, but independent of bone density. Based on the velocity and amplitude of the received waves, equations were proposed to estimate the bone elasticity and bone density [111]. The study has shown significant correlation of such measurements with those obtained by peripheral quantitative computerized tomography for an Asian

population (n = 52) [112].

Backscatter Processing Ultrasound systems also obtain quantitative measurements by processing the backscattered waves. In pulse mode, ultrasound echoes of cancellous bone come from interfaces among the solid trabecular network (rod-like or plate-like) and the marrow. Therefore, they are composed of multiple interfering contributions due to random scatters. The backscattered signal also depends on the ultrasound wavelength, geometry and orientation of the trabecular structures relative to the incident wave. Several quantitative indices obtained from backscattered ultrasound have been proposed to characterize bone density and microstructure [108]. *In vivo* measurements have shown moderate correlation between proposed backscatter indices and BMD measured by DXA [113,114]. Based on backscatter indices, ultrasound parametric imaging for *ex vivo* bone samples has been investigated [115].

Ultrasound medical images are built based on echoes originated from tissue boundaries at different body depths; brightness of image pixels are associated to amplitudes of the returned echoes. For two dimensional visualization of a given anatomical structure, the ultrasound system scans consecutive body slices. The radiofrequency echographic multi-spectrometry (REMS) system generates conventional images and stores the unprocessed backscattered (also called radiofrequency - RF) signals from 100 scans (frames) of the interrogated body region; usually, lumbar spine (L1-L4) or femoral neck. Custom-implemented algorithms automatically identify signals backscattered from the vertebrae and select an analysis region using a spectral model database as reference. Next, spectra of the patient's RF signals are compared to those of age-matched models (51-55 and 56-60 years old) previously classified by means of DXA as osteoporotic, osteopenic or healthy [116]. Studies carried out for Caucasian populations (n< 1640) showed good performance of REMS measurements when compared to those obtained by DXA [117,118]. The European Society for Clinical and Economic Aspects of Osteoporosis, osteoarthritis and musculoskeletal diseases (ESCEO) states that the REMS has the potential to become the first clinically available method for direct non-ionizing measurement of lumbar and femoral BMD [119].

3.5. Clinical Tools

BMD measured by DXA has low sensitivity to assess fracture risk since other factors are involved. The fracture risk assessment tool (FRAX is a computer-based algorithm that, based on multiple clinical risk factors, estimates the 10-year probability of a major fracture (hip, vertebrae, humerus or wrist fracture)). The risk factors are previous fragility fracture, parental hip fracture, smoking, systemic glucocorticoid intake, excessive alcohol consumption, rheumatoid arthritis, and secondary causes of osteoporosis (e.g., type I diabetes, chronic malnutrition, endocrine disorders); besides, age, sex, and BMI are taken into account. BMD measured from the femoral neck may also be used as an optional input. The fracture probability also involves the risk of death [120,121]. FRAX has low cost and may be used where other methods are not available.

FRAX, first released in 2008, has 71 models based on the epidemiology of fractures adapted for 66 countries. It is a tool recommended in more than 80 osteoporosis prevention guidelines around the world [120–123].

FRAX algorithm has been improved over the time. There were adjustments to calibrate the results according to the time passed by after a fracture, since evidences indicate an increased risk of a new fracture after a recent one. Recently, an additional category, very high-risk, was included due to development of new treatment options. Thus, more modern and efficient drugs (anabolic therapy) may be prescribed for such patients while the high-risk patients continue receiving conventional drugs [124].

For example, the UK NOGG recommends major osteoporotic fracture (MOF) assessment of postmenopausal women, and men age 50 years or older by means of FRAX to classify patients in four risk groups: low,
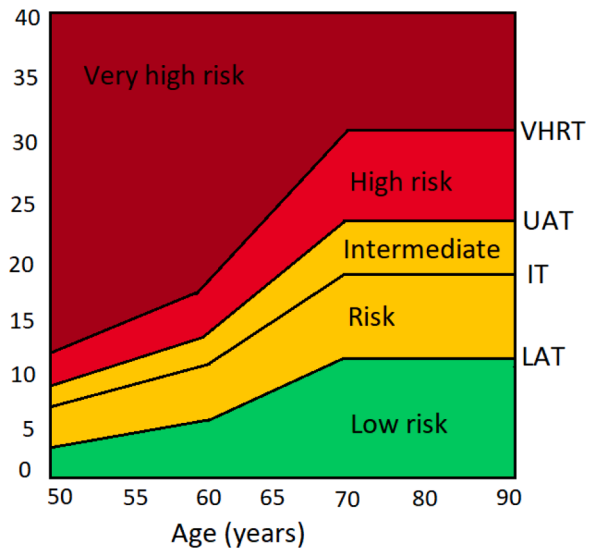
Fig. 4. UK NOGG recommendations of assessment, intervention, and risk thresholds for major osteoporotic fracture probability (MOF) using FRAX. The four thresholds are: VHRT (Very high risk), UAT (Upper assessment), IT (Intervention), and LAT (Lower assessment threshold). Modified from [37].

intermediate, high, and very high (Fig 4). Those with FRAX probabilities of 10-year MOF risk above UAT (high and very high risk patients), shall have their BMD measured to guide drug choice and provide a baseline for BMD monitoring. Those classified as intermediate risk patients (between UAT and LAT) are further assessed with BMD measurement; if new calculated probabilities using BMD lie above or below intervention (IT), it is recommended treatment or given lifestyle advice, respectively. If BMD measurements are not viable, intermediate risk patients with probabilities above IT are considered for treatment. Low risk patients do not require BMD measurements and shall modify their lifestyle [37].

FRAX has also some limitations. Owing to its dependence on different preventive therapies, there is no universal pattern to assess its results [121,125]. It fails in computing the impact of different exposure periods to some risk factors (e.g. the amount and time of glucocorticoids intake) which leads to different outcomes [121,126,127]. There is a large number of other fracture risk factors that are not taken into account by FRAX.

Aiming to circumvent that, several clinical tools have been proposed [128]. Garvan, for instance, was developed for the Australian population and Qfracture for the British one. Studies suggest their potential
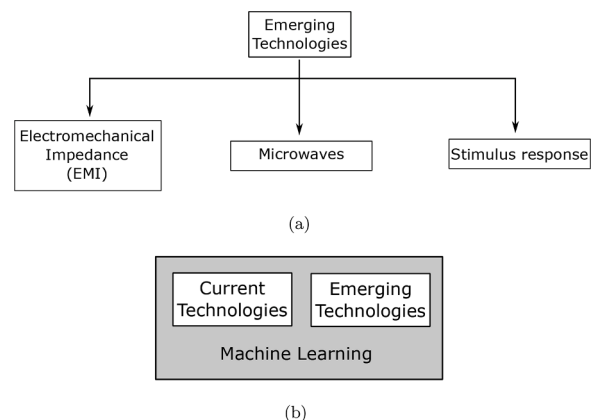
Fig. 5. Emerging technologies. a) Scheme of the emerging technologies for osteoporosis diagnosis, b) machine learning as a tool for osteoporosis diagnosis.

applicability. However, both tools have limitations, since they have not been adapted for populations different from those comprised in their development. Comparison among these tools is difficult due to substantial differences among their inputs and outputs. Thus, additional evidences are needed to support or reject their wide application [129–131].

4. Emerging Technologies

Emerging technologies have been proposed to ease osteoporosis diagnosis with the premises of being cost-effective, portable, and reduce power consumption. The techniques assess responses from bones after the application of stimuli/excitation. These methods are described in the next subsections following the structure of Fig 5.

4.1. Electromechanical Impedance-based Methods

The electromechanical impedance (EMI) technique detects failures of structures in a wide range of applications (mechanical, civil, aerospace, marine, and others), being first proposed by Liang *et al.* in 1994 [132].

A low amplitude voltage is applied to a piezoelectric lead zirconate titanate sensor (PZT) bonded to the structure of interest in order to evaluate their coupling. Application of a sinusoidal voltage ($U = Um \cdot e^{jwt}$) to the PZT patch generates a current ($I = Im \cdot e^{(jwt+\theta)}$), being the electrical impedance of the PZT obtained by [132]:

$$Z_E(\omega) = \frac{U}{I} = \frac{1}{j\omega a}\left(\bar{\epsilon}_{33}^T - \frac{Z(\omega)}{Z(\omega) + Z_a(\omega)}d_{3x}^2 Y_{xx}^E\right)^{-1} \qquad (2)$$

where j, $Z_a(\omega)$, $Z(\omega)$, $\bar{\epsilon}_{33}^T$, d_{3x}^2, Y_{xx}^E and a correspond to imaginary unit, transducer impedance, monitored structure impedance, electric field constant, coupling piezoelectric constant, Young's modulus of the monitored structure, and geometric constant, respectively. Thus, modification of the monitored structure impedance is followed by electrical impedance changes of the PZT. EMI has been widely applied for structural health monitoring (SHM), since PZT transducers are inexpensive.

The interaction between the applied voltage signal and the structure under study generates resonant peaks at different frequencies. The resonant frequencies and their amplitudes are affected by structural damages. Resonant frequencies are very sensitive to geometry, mass, boundary conditions or even external effects (temperature and sensor placement). Low frequency signals have large wavelengths that provide global information about the structure; that is, detection of significant damages (or bone fractures in the current context). On the other hand, high frequency signals (short wavelengths) are more prone to detect small damages. However, such systems shall have repeatability to be useful [133].

In practice, a function generator applies a sinusoidal voltage signal to the PZT, sweeping different frequencies in order to obtain the frequency response function (FRF); the so-called EMI signature. Several electronic devices have been developed to acquire EMI signatures [134,135]. EMI technique has low-cost and portability.

4.1.1. EMI Applied to Bone Assessment

In the osteoporosis context, EMI application requires the placement of PZT patch on the bone (surrounded by skin, muscles, and fat) to measure the coupling parameters that are likely related to the tissues properties.

EMI based methods demand a reference signature (baseline); in this context, it should be obtained from healthy bones. Later, signal processing techniques are applied to a sampled EMI signature in order to extract the most significant features that are compared to the baseline. Any deviation from the baseline may be analyzed as a bone related condition [136]. Generally, statistical methods are used to classify the signature as a healthy or osteoporotic. Root mean square deviation (RMSD) and correlation coefficient deviation metric (CCDM) have been recurrently employed for this purpose [137].

4.1.2. Current Stage

To date, there are few reports on the evaluation of bone's health by EMI based methods. In [138], the authors used two PZT patches to investigate bone cracks in *ex vivo* animal model; shifts of the FRF peaks due to damages were detected. In [139], the authors investigated EMI applied to an *ex vivo* human femur with fissure and fracture as well as the effect of density increase due to wetting of dry bone. In [140], EMI based method was able to detect artificially induced bone fissures. Experimental results were analyzed by quantifying RMSD computed between EMI frequency responses obtained from bone with and without fissures. The results showed that the EMI detects structural changes of bones.

In [137], the authors simulated osteoporosis in an *ex vivo* bovine bone by drilling various small holes in it. Changes of the resonant frequencies measured before and after drilling the bone were investigated. Furthermore, the authors investigated two methods for fixing PZTs on the bones: bonded sensor (BS) and non-bonded sensor (NBS). The BS is directly glued to the bone. NBS is kept on the bone by means of clamps. Modifications of the resonant frequencies occurs as the torque of the clamp screws changes, affecting the results of the analysis. In [141], the authors proposed an autonomous gripping mechanism for NBS using shape memory alloy (SMA) wires. In summary, they replaced the clamps by SMA wires to fix the PZT on the bone. Experiments were performed on *ex vivo* healthy and osteoporotic femur bones with promising results. In [142], the authors assessed NBS and BS with finite element models of the radius and femur; they concluded that the simulations matched well the experimental results of their previous investigations [137,141,143].

From the reported studies, EMI based methods sound promising. However, there are technical challenges for their clinical use. Application pressure of PZT transducers on the body, frequency range for *in vivo* measurements, *in vivo* characterization of healthy and osteoporotic bones, validation of quantitative indices are aspects that require further investigation to assess their potential for bone health assessment.

4.2. Stimulus Response-based Methods

To diagnose osteoporosis, researchers have also investigated the vibration of bones resulting from mechanical stimulus. For that, an impulsive stimulus (using a vibration hammer, electromechanical devices, and others) is applied to bone (radius or tibia); at some axial distance, the propagated wave is sampled by means of a sensor (stethoscope, accelerometers, and others). Methods based on such premise take into account that the bone's lowest fundamental natural frequency (f_0) is closely related to its stiffness.

Statistical signal processing methods are applied to extract osteoporosis sensitive features from the sampled waveforms that are associated to bone health.

Bone elastic responses have been investigated since early 70s [144]. For concision, this review focuses on recent approaches. In [145], an instrumented vibration hammer is used to stimulate the bone (tibia), the resulting vibration is picked up by accelerometers. Similar procedures were carried out in [146,147]. Methods based on vibroacoustic are very sensitive to geometry, mass, boundary conditions or even external effects (noise, temperature, and sensor placement), thereby hampering the follow-up of osteoporosis treatment [144,148]. The impact of the mass on the natural frequency is greater than stiffness. Muscles damp the vibrations; thus, they shall be added to the whole system mass. Effects due to fibula and joints are difficult to quantify. The bone length has a minor effect on the bone natural frequency [149]. In [148], electronic stethoscope was used to acquire bone's response instead of an accelerometer. Broadly, researchers' findings showed that bone strength is not always associated to mineral density since the bone may have a fragile section [145]. The low cost and portability of such systems make them

very attractive for osteoporosis screening. However, the impact of physical characteristics (BMI, soft tissue composition, and joints) on the measured response may be very difficult to circumvent.

4.3. Microwave Frequency-based Methods

Dielectric properties of bones over microwave frequency bandwidth have been investigated to characterize osteoporosis from volunteers [150] and *ex-vivo* samples [151]. Recently, a device was designed for such purpose [152] consisting of antennas (5cm x 1.8cm) placed on opposite sides of the wrist under controlled pressure (1kg.f). The wrist was chosen because it is more easily accessed without being surrounded by large amount of soft tissues. The setup radiates 0.1 W of RF (30kHz to 2GHz) to the wrist without requiring an impedance matching medium (gel or water). The microwave transmission coefficient ($s_{21}(f)$), affected by attenuation and scattering, was measured from healthy (n=37) and osteopenic/osteoporotic subjects (n=23); the volunteers were 23-94 years old, being 48 female and 12 male. They were classified as osteopenic or osteoporotic based on T-score (DXA) measurements or clinical history. The authors concluded that their results correlate well with the disease classification (86% for female; 100% for male), being safer and less expensive.

As other emerging technologies, more clinical studies are necessary to validate the potential of such proposals to assist the diagnosis of osteoporosis.

4.4. Machine Learning-based Methods

Due to the significant increment of machine learning applications in medical sciences, a brief section on the use of such tools on osteoporosis diagnosis is presented.

Machine learning involves computer algorithms that search, with little or without human intervention, patterns in sampled data to allow, for instance, predictions or their classification into different categories. Detailed description of these algorithms may be found elsewhere [153, 154].

Since osteoporosis is a multi-factorial disease, machine learning algorithms have been taking into account clinical risk factors (malnutrition, previous fracture, previous diseases, medications, ethnicity, heredity, alcohol consumption, and others) and anthropometric data (sex, age, height, weight, and others) in order to outperform clinical tools (such as FRAX) in the prediction of fractures [155,156].

As a matter of fact, machine learning has been applied to a large diversity of scenarios (BMD data, dental radiographs, QCT measurements, and others) to assist diagnosis of osteoporosis, having deserved recent reviews entirely dedicated to this subject [157,158]. For instance, it has been used for the automatic detection of boundaries in bone images (obtained by means of x-rays, DXA, CT, and MRI), delimiting sections with similar characteristics (image segmentation); after the image segmentation, features are extracted from those sections to be used by classifiers (such as machine learning algorithms) to detect osteoporosis [159].

Machine learning is a transversal tool that may complement any of the presented technologies (Figure 5(b)). The measurements of the existing technologies may be processed to enhance the diagnosis as well as assist the interpretation of the results, revealing underlying patterns and grounds of the osteoporosis diagnosis.

Despite the large number of investigations, additional research will be necessary to consolidate its potential in such applications.

5. Challenges and Conclusions

Population aging demands the development of new technologies to improve treatment of the associated illnesses in order to reduce health costs and assure quality of life. In this context, new methods to support osteoporosis management would have a significant impact, since its

Table 1
Current applied technologies: capabilities and limitations.

Technology	Capabilities	Limitations	References
Dual-X-Ray Absorptiometry (DXA)			
• Based on X-rays	• Gold standard for diagnosis • Independent diagnosis	• Requires rigorous quality control procedures • Expensive, large, and bulky • Inaccurate measurements in bones affected by desmophytes or previously fractured • Patient's exposure to ionizing radiation • Absence of reference indices (T-score, Z-score) for populations with large racial diversity • Questionable adequacy for follow-up	[22,29,30]
Vertebral Fracture Assessment			
• DXA based method • Analyses of lateral spine images	• Complements DXA • Radiation dose 200 times lower than standard X-ray devices	• Applicable only in association with DXA • Patient's exposure to ionizing radiation • Qualitative assessment	[34,36]
Trabecular Bone Score			
• DXA based method • Image gray scale analysis	• Complements DXA • Accuracy unaffected by presence of desmophytes	• Not suitable for follow-up • Requires complementary exams • Patient's exposure to ionizing radiation	[47–49, 160]
Quantitative-Computed Tomography			
• Based on X-rays • Generates multiple cross sectional images • Analyses quantitative parameters	• Less susceptible to confounding factors • Higher sensitivity than DXA • Quantitative and qualitative assessment	• High ionizing radiation exposure • High cost and low availability • Complex scanning procedure	[26,55,59, 61]
Peripheral QCT			
• Computed Tomography based method • Applied to appendicular skeleton sites	• Less bulky, less expensive, lower radiation and higher mobility than QCT • Better follow-up	• High cost • Patient's exposure to ionizing radiation	[55,73,75, 78,152]
Magnetic Resonance Imaging			
• Images based on RF signals emitted by hydrogen atoms excited by magnetic fields	• Ionizing radiation free	• Expensive • Time consuming	[82,85,86]

(continued on next page)

Table 1 (*continued*)

Technology	Capabilities	Limitations	References
Quantitative Ultrasound			
• Piezoelectric transducers	• Ionizing radiation free	• Results discrepancy among devices	[97–99, 106,112, 117–119]
• Assesses properties of ultrasound waves applied to the bones	• Low cost and portable	• Not suitable for diagnosis	
	• Useful for screening	• Not suitable for follow-up	
Clinical tools			
• Computer-based algorithm	• Low cost	• Each proposed tool has different inputs and outputs	[120,121, 126,127, 129–131, 161]
• Fracture risk assessment based on risk factors	• Offers independent fractures risk assessment	• Not suitable for follow-up	
	• Comprises several risk factors	• Not validated for all different populations	

Table 2

Emerging technologies: capabilities and limitations.

Technology	Capabilities	Limitations	References
Electromechanical Impedance			
• Based on electrical impedance measurement • Use low cost PZT patches • Requires a reference measurement (baseline)	• Ionizing radiation free • Low cost • Portable • Easy handling	• No consistent quantitative results • Limitation to place PZT patch on bones • Affected by boundary conditions	[137,141, 142]
Stimulus Response			
• Based on the vibration theory • Measures bone response resulting from mechanical stimulus	• Ionizing radiation free • Low cost • Portable • Easy handling	• No consistent quantitative results • Affected by boundary conditions	[146,147]
Microwave frequency			
• Based on radio wave propagation • Uses on-body antennas • Applied to the wrist	• Ionizing radiation free • Low radiated power (0.1 W) • No need of coupling media • Easy handling • Fast response (2030s)	• Requires additional clinical studies	[152]
Machine Learning			
• Based on computer algorithms • Extracts and classifies patterns	• Assesses clinical risk factors • Classifies patterns without human intervention • Analyzes other techniques' measurements	• Affected by quality of data input • Affected by coding quality • Above aspects hamper comparisons	[152]

incidence starts at relative early ages. The main challenge is to develop a technology that provides an accurate diagnosis at low cost such that low income countries may also benefit from it. An additional requirement is that such technology may be enclosed into a portable device; thus, isolated populations could also be assisted. Reliability of quantitative indices to support diagnosis is also important; thus, the technology becomes independent of expert examiners' availability.

A summary of related critical aspects, capabilities and limitations, for both current applied (Table 1) and emerging technologies (Table 2), are depicted.

Previous sections reviewed the most applied technologies for osteoporosis diagnosis. Nowadays, such condition is mainly diagnosed based on BMD measurements obtained by means of DXA. However, its potential to identify fractures risk has been questioned. Furthermore, it requires the patients' exposure to ionizing radiation.

New technologies have been proposed for such purpose, aiming to provide alternatives to DXA as well as reliable quantitative indices to improve diagnosis. However, some investigated methods increase the patients' exposure to ionizing radiation (QCT, pQCT, HR-pQCT), have no mobility and high costs (QCT, pQCT, HR-pQCT, and MRI). It should be emphasized that such methods are very useful as research tools to investigate osteoporosis as well as for opportunistic screening; however, even if they become the gold standard, there will be need to develop other technologies that may be less expensive and portable.

QUS systems do not apply ionizing radiation, have portability and relative low cost. Due to these characteristics, they may replace DXA devices in the near future. There are several commercial systems in the market, but the manufactures need to circumvent some technological challenges in order to have their devices recommended by health surveillance agencies.

Majority of these technological approaches have been compared to DXA results, demonstrating utility for a complementary analysis of osteoporosis. These methods aim to characterize bone fragility, but they do not assess fracture risk. For such purpose, clinical tools have been proposed. FRAX is the most applied, being a computer-based algorithm that takes into accounts multiple clinical risk factors to estimate a 10-year probability of a major fracture. It is a tool recommended by several prevention guidelines around the world, but it does not take into account many risk factors and it may not have a good performance in countries with a large ethnic diversity. Such tools depend on medical records or patients' collaboration. Thus, despite further development, the clinical tools can not always replace complementary diagnostic exams.

Although emerging technologies have presented promising preliminary results, they demand further investigations to prove their potential to assist osteoporosis diagnosis.

The basic premise of this publication is to collate information about the current and emerging technologies for osteoporosis screening. Such overview may guide the choice of technology for different research and clinical scenarios. This publication also shows the challenges to achieve a low cost, robust, portable and reliable method for diagnosis and follow-up of osteoporosis treatment.

Declaration of Competing Interest

None declared.

Ethical approval

Not required.

Acknowledgement

References

[1] Cooper C, Campion G, Melton LJr. Hip fractures in the elderly: a world-wide projection. Osteoporosis international 1992;2(6):285–9.

[2] Wright NC, Saag KG, Dawson-Hughes B, Khosla S, Siris ES. The impact of the new national bone health alliance (NBHA) diagnostic criteria on the prevalence of osteoporosis in the USA. Osteoporosis International 2017;28(4):1225–32.

[3] Borgström F, Karlsson L, Ortsäter G, Norton N, Halbout P, Cooper C, Lorentzon M, McCloskey EV, Harvey NC, Javaid MK, et al. Fragility fractures in europe: burden, management and opportunities. Archives of osteoporosis 2020;15(1):1–21.

[4] Cheng X, Dong S, Wang L, Feng J, Sun DM, Zhang Q, Huang JY, Wen QX, Hu R, Li N, et al. Prevalence of osteoporosis in china: a multicenter, large-scale survey of a health checkup population. Chin J Health Manage 2019;13:51–8.

[5] Siqueira FV, Facchini LA, Hallal PC. The burden of fractures in brazil: a population-based study. Bone 2005;37(2):261–6.

[6] Fox KM, Cummings SR. Is tubal ligation a risk factor for low bone density and increased risk of fracture? American journal of obstetrics and gynecology 1995; 172(1):101–5.

[7] IOF. BROKEN BONES, BROKEN LIVES: A roadmap to solve the fragility fracture crisis in Europe. Tech. Rep. International Osteoporosis Foundation; 2018.

[8] Carey JJ, Buehring B. Current imaging techniques in osteoporosis. Clin Exp Rheumatol 2018;36(114):5.

[9] Morgan EF, Unnikrisnan GU, Hussein AI. Bone mechanical properties in healthy and diseased states. Annual review of biomedical engineering 2018;20:119–43.

[10] Keaveny TM, Morgan EF, Niebur GL, Yeh OC. Biomechanics of trabecular bone. Annual review of biomedical engineering 2001;3(1):307–33.

[11] Choksi P, Jepsen KJ, Clines GA. The challenges of diagnosing osteoporosis and the limitations of currently available tools. Clinical diabetes and endocrinology 2018; 4(1):12.

[12] Florencio-Silva R, Sasso GRdS, Sasso-Cerri E, Simões MJ, Cerri PS. Biology of bone tissue: structure, function, and factors that influence bone cells. BioMed research international 2015;2015.

[13] Prevention WSGo, Osteoporosis Mo, Organization WH. Prevention and management of osteoporosis: report of a WHO scientific group. World Health Organization; 2003.

[14] Komar C, Ahmed M, Chen A, Richwine H, Zia N, Nazar A, Bauer L. Advancing methods of assessing bone quality to expand screening for osteoporosis. J Am Osteopath Assoc 2019;119:147–54.

[15] Crandall CJ, Ensrud KE. Osteoporosis screening in younger postmenopausal women. Jama 2020;323(4):367–8.

[16] Buckley L, Humphrey MB. Glucocorticoid-induced osteoporosis. New England Journal of Medicine 2018;379(26):2547–56.

[17] Szulc P, Bouxsein ML. Overview of osteoporosis: epidemiology and clinical management. Vertebral fracture initiative resource document 2011.

[18] Cosman F, de Beur SJ, LeBoff MS, Lewiecki EM, Tanner B, Randall S, Lindsay R. Clinicians guide to prevention and treatment of osteoporosis. Osteoporosis international 2014;25(10):2359–81.

[19] Camacho PM, Petak SM, Binkley N, Clarke BL, Harris ST, Hurley DL, Kleerekoper M, Lewiecki EM, Miller PD, Narula HS, et al. American association of clinical endocrinologists and american college of endocrinology clinical practice guidelines for the diagnosis and treatment of postmenopausal osteoporosis2016. Endocrine Practice 2016;22(s4):1–42.

[20] Radominski SaC, Bernardo W, Paula APd, Albergaria B-H, Moreira C, Fernandes CE, Castro CHM, de Freitas ZCA, Domiciano DS, Mendonca L, et al. Brazilian guidelines for the diagnosis and treatment of postmenopausal osteoporosis. Revista brasileira de reumatologia 2017;57:s452–66.

[21] Leslie WD, Adler RA, Fuleihan GE-H, Hodsman A, Kendler DL, McClung M, Miller PD, Watts NB. Application of the 1994 WHO classification to populations other than postmenopausal caucasian women: the 2005 ISCD official positions. Journal of Clinical Densitometry 2006;9(1):22–30.

[22] Kanis JA, Cooper C, Rizzoli R, Reginster J-Y. Correction to: European guidance for the diagnosis and management of osteoporosis in postmenopausal women. Osteoporosis International 2020;31(4).801–801

[23] Lee RL, Dacre JE, James MF. Image processing assessment of femoral osteopenia. Journal of digital imaging 1997;10(1):218–21.

[24] Harvey NC, McCloskey E, Kanis JA, Compston J, Cooper C. Cost-effective but clinically inappropriate: new NICE intervention thresholds in osteoporosis (technology appraisal 464). Osteoporosis International 2018;29(7):1511–3.

[25] Aggarwal V, Maslen C, Abel RL, Bhattacharya P, Bromiley PA, Clark EM, Compston JE, Crabtree N, Gregory JS, Kariki EP, et al. Opportunistic diagnosis of osteoporosis, fragile bone strength and vertebral fractures from routine CT scans; a review of approved technology systems and pathways to implementation. Therapeutic advances in musculoskeletal disease 2021;13.1759720X211024029

[26] Schultz K, Wolf JM. Emerging technologies in osteoporosis diagnosis. The Journal of hand surgery 2019;44(3):240–3.

[27] Messina C, Albano D, Gitto S, Tofanelli L, Bazzocchi A, Ulivieri FM, Guglielmi G, Sconfienza LM. Body composition with dual energy x-ray absorptiometry: from basics to new tools. Quantitative Imaging in Medicine and Surgery 2020;10(8): 1687.

[28] Shuhart CR, Yeap SS, Anderson PA, Jankowski LG, Lewiecki EM, Morse LR, Rosen HN, Weber DR, Zemel BS, Shepherd JA. Executive summary of the 2019 ISCD position development conference on monitoring treatment, DXA cross-calibration and least significant change, spinal cord injury, peri-prosthetic and orthopedic bone health, transgender medicine, and pediatrics. Journal of Clinical Densitometry 2019;22(4):453–71.

[29] Carey JJ, Delaney MF. Utility of DXA for monitoring, technical aspects of DXA BMD measurement and precision testing. Bone 2017;104:44–53.

[30] Qaseem A, Forciea MA, McLean RM, Denberg TD. Treatment of low bone density or osteoporosis to prevent fractures in men and women: a clinical practice guideline update from the american college of physicians. Annals of internal medicine 2017;166(11):818–39.

[31] Aldieri A, Terzini M, Osella G, Priola AM, Angeli A, Veltri A, Audenino AL, Bignardi C. Osteoporotic hip fracture prediction: is t-score-based criterion enough? a hip structural analysis-based model. Journal of biomechanical engineering 2018;140(11).

[32] Shin YH, Gong HS, Kim KM, Lee JH, Kwon O, Baek GH. Evaluation of hip geometry parameters in patients with a distal radius fracture. Journal of Clinical Densitometry 2020;23(4):576–81.

[33] Aldieri A, Terzini M, Audenino AL, Bignardi C, Morbiducci U. Combining shape and intensity dxa-based statistical approaches for osteoporotic HIP fracture risk assessment. Computers in Biology and Medicine 2020;127:104093.

[34] Borges JLC, da Silva MS, Ward RJ, Diemer KM, Yeap SS, Lewiecki EM. Repeating vertebral fracture assessment: 2019 ISCD official position. Journal of Clinical Densitometry 2019;22(4):484–8.

[35] Prince RL, Lewis JR, Lim WH, Wong G, Wilson KE, Khoo BC, Zhu K, Kiel DP, Schousboe JT. Adding lateral spine imaging for vertebral fractures to densitometric screening: improving ascertainment of patients at high risk of incident osteoporotic fractures. Journal of Bone and Mineral Research 2019;34 (2):282–9.

[36] Schousboe JT, Lix LM, Morin SN, Derkatch S, Bryanton M, Alhrbi M, Leslie WD. Vertebral fracture assessment increases use of pharmacologic therapy for fracture prevention in clinical practice. Journal of Bone and Mineral Research 2019;34 (12):2205–12.

[37] Gregson CL, Armstrong DJ, Bowden J, Cooper C, Edwards J, Gittoes NJL, Harvey N, Kanis J, Leyland S, Low R, et al. Uk clinical guideline for the prevention and treatment of osteoporosis. Archives of osteoporosis 2022;17(1): 1–46.

[38] Hans D, Šteňová E, Lamy O. The trabecular bone score (TBS) complements DXA and the FRAX as a fracture risk assessment tool in routine clinical practice. Current osteoporosis reports 2017;15(6):521–31.

[39] Martineau P, Silva BC, Leslie WD. Utility of trabecular bone score in the evaluation of osteoporosis. Current Opinion in Endocrinology & Diabetes and Obesity 2017;24(6):402–10.

[40] Martineau P, Leslie WD. Trabecular bone score (TBS): Method and applications. Bone 2017;104:66–72.

[41] Martineau P, Leslie WD, Johansson H, Harvey NC, McCloskey EV, Hans D, Kanis JA. In which patients does lumbar spine trabecular bone score (TBS) have the largest effect? Bone 2018;113:161–8.

[42] Borgen TT, Bjørnerem A, Solberg LB, Andreasen C, Brunborg C, Stenbro M-B, Hübschle LM, Figved W, Apalset EM, Gjertsen J-E, et al. Determinants of trabecular bone score and prevalent vertebral fractures in women with fragility fractures: a cross-sectional sub-study of noFRACT. Osteoporosis International 2020;31(3):505–14.

[43] Olmos JM, Hernández JL, Pariente E, Martínez J, Valero C, González-Macías J. Trabecular bone score and bone quantitative ultrasound in spanish postmenopausal women. the camargo cohort study. Maturitas 2020;132:24–9.

[44] Silva BC, Broy SB, Boutroy S, Schousboe JT, Shepherd JA, Leslie WD. Fracture risk prediction by non-BMD DXA measures: the 2015 ISCD official positions part 2: trabecular bone score. Journal of Clinical Densitometry 2015;18(3):309–30.

[45] Harvey NC, Glüer CC, Binkley N, McCloskey EV, Brandi M-L, Cooper C, Kendler D, Lamy O, Laslop A, Camargos BM, et al. Trabecular bone score (TBS) as a new complementary approach for osteoporosis evaluation in clinical practice. Bone 2015;78:216–24.

[46] McCloskey EV, Odén A, Harvey NC, Leslie WD, Hans D, Johansson H, Barkmann R, Boutroy S, Brown J, Chapurlat R, et al. A meta-analysis of trabecular bone score in fracture risk prediction and its relationship to FRAX. Journal of bone and mineral research 2016;31(5):940–8.

[47] Padlina I, Gonzalez-Rodriguez E, Hans D, Metzger M, Stoll D, Aubry-Rozier B, Lamy O. The lumbar spine age-related degenerative disease influences the BMD not the TBS: the osteolaus cohort. Osteoporosis international 2017;28(3):909–15.

[48] Kolta S, Briot K, Fechtenbaum J, Paternotte S, Armbrecht G, Felsenberg D, Glüer CC, Eastell R, Roux C. Tbs result is not affected by lumbar spine osteoarthritis. Osteoporosis International 2014;25(6):1759–64.

[49] Sooragonda B, Cherian KE, Jebasingh FK, Dasgupta R, Asha HS, Kapoor N, Thomas N, Paul TV. Longitudinal changes in bone mineral density and trabecular bone score following yearly zoledronic acid infusion in postmenopausal osteoporosisa retrospective-prospective study from southern india. Archives of osteoporosis 2019;14(1):79.

[50] Jowita H-Z, Gojny L, Bolanowski M. Trabecular bone score (TBS) as a noninvasive and complementary tool for clinical diagnosis of bone structure in endocrine disorders. Endokrynologia Polska 2019;70(4):350–6.

[51] Jiang N, Xia W. Assessment of bone quality in patients with diabetes mellitus. Osteoporosis International 2018;29(8):1721–36.

[52] Anderson KB, Holloway-Kew KL, Mohebbi M, Kotowicz MA, Hans D, Pasco JA. Is trabecular bone score less affected by degenerative-changes at the spine than lumbar spine BMD? Archives of osteoporosis 2018;13(1):127.

[53] Hathcock JT, Stickle RL. Principles and concepts of computed tomography. Veterinary Clinics of North America: Small Animal Practice 1993;23(2):399–415.

[54] Rietzel E, Pan T, Chen GTY. Four-dimensional computed tomography: image formation and clinical protocol. Medical physics 2005;32(4):874–89.

[55] Engelke K, Adams JE, Armbrecht G, Augat P, Bogado CE, Bouxsein ML, Felsenberg D, Ito M, Prevrhal S, Hans DB, et al. Clinical use of quantitative computed tomography and peripheral quantitative computed tomography in the management of osteoporosis in adults: the 2007 ISCD official positions. Journal of clinical densitometry 2008;11(1):123–62.

[56] Guerri S, Mercatelli D, Gómez MPA, Napoli A, Battista G, Guglielmi G, Bazzocchi A. Quantitative imaging techniques for the assessment of osteoporosis and sarcopenia. Quantitative imaging in medicine and surgery 2018;8(1):60.

[57] Mookiah MRK, Rohrmeier A, Dieckmeyer M, Mei K, Kopp FK, Noel PB, Kirschke JS, Baum T, Subburaj K. Feasibility of opportunistic osteoporosis screening in routine contrast-enhanced multi detector computed tomography (MDCT) using texture analysis. Osteoporosis International 2018;29(4):825–35.

[58] Johannesdottir F, Allaire B, Kopperdahl DL, Keaveny TM, Sigurdsson S, Bredella MA, Anderson DE, Samelson EJ, Kiel DP, Gudnason VG, et al. Bone density and strength from thoracic and lumbar CT scans both predict incident vertebral fractures independently of fracture location. Osteoporosis International 2021;32(2):261–9.

[59] Nam KH, Seo I, Kim DH, Lee JI, Choi BK, Han IH. Machine learning model to predict osteoporotic spine with hounsfield units on lumbar computed tomography. Journal of Korean Neurosurgical Society 2019;62(4):442.

[60] Genant HK, Block JE, Steiger P, Glueer C-C, Smith R. Quantitative computed tomography in assessment of osteoporosis. Seminars in nuclear medicine. vol. 17. Elsevier; 1987. p. 316–33.

[61] Pan Y, Shi D, Wang H, Chen T, Cui D, Cheng X, Lu Y. Automatic opportunistic osteoporosis screening using low-dose chest computed tomography scans obtained for lung cancer screening. European Radiology 2020:1–10.

[62] Paggiosi MA, Debono M, Walsh JS, Peel N, Eastell R. Quantitative computed tomography discriminates between postmenopausal women with low spine bone mineral density with vertebral fractures and those with low spine bone mineral density only: the SHATTER study. Osteoporosis International 2020:1–9.

[63] Terzini M, Aldieri A, Rinaudo L, Osella G, Audenino AL, Bignardi C. Improving the hip fracture risk prediction through 2d finite element models from DXA images: validation against 3d models. Frontiers in bioengineering and biotechnology 2019;7:220.

[64] Pickhardt PJ, Pooler BD, Lauder T, del Rio AMn, Bruce RJ, Binkley N. Opportunistic screening for osteoporosis using abdominal computed tomography scans obtained for other indications. Annals of internal medicine 2013;158(8):588–95.

[65] Dagan N, Elnekave E, Barda N, Bregman-Amitai O, Bar A, Orlovsky M, Bachmat E, Balicer RD. Automated opportunistic osteoporotic fracture risk assessment using computed tomography scans to aid in FRAX underutilization. Nature Medicine 2020;26(1):77–82.

[66] Li Y, Zhao Z, Wang L, Fu Z, Ji L, Wu X. The prevalence of osteoporosis tested by quantitative computed tomography in patients with different glucose tolerances. The Journal of Clinical Endocrinology & Metabolism 2020;105(1):201–9.

[67] Aldieri A, Bhattacharya P, Paggiosi M, Eastell R, Audenino AL, Bignardi C, Morbiducci U, Terzini M. Improving the hip fracture risk prediction with a statistical shape-and-intensity model of the proximal femur. Annals of biomedical engineering 2022;50(2):211–21.

[68] McDonald AM, Yang ES, Saag KG, Levitan EB, Wright NC, Fiveash JB, Rais-Bahrami S, Bhatia S. Osteoporosis screening using computed tomography for men with prostate cancer: results of a prospective study. Archives of Osteoporosis 2020;15(1):1–7.

[69] Pisu M, Kopperdahl DL, Lewis CE, Saag KG, Keaveny TM. Cost-effectiveness of osteoporosis screening using biomechanical computed tomography for patients with a previous abdominal CT. Journal of Bone and Mineral Research 2019;34(7):1229–39.

[70] Keaveny TM, Clarke BL, Cosman F, Orwoll ES, Siris ES, Khosla S, Bouxsein ML. Biomechanical computed tomography analysis (BCT) for clinical assessment of osteoporosis. Osteoporosis International 2020:1–24.

[71] Koh K-J, Kim K-A. Utility of the computed tomography indices on cone beam computed tomography images in the diagnosis of osteoporosis in women. Imaging science in dentistry 2011;41(3):101–6.

[72] de Castro JGK, Carvalho BF, de Melo NS, de Souza Figueiredo PT, Moreira-Mesquita CR, de Faria Vasconcelos K, Jacobs R, Leite AF. A new cone-beam computed tomography–driven index for osteoporosis prediction. Clinical Oral Investigations 2020:1–10.

[73] Augat P, Eckstein F. Quantitative imaging of musculoskeletal tissue. Annu Rev Biomed Eng 2008;10:369–90.

[74] Makarov SN, Noetscher GM, Arum S, Rabiner R, Nazarian A, et al. The impact of the new national bone health alliance (NBHA) diagnostic criteria on the prevalence of osteoporosis in the USA. Osteoporosis International 2020;31(1):216–24.

[75] Schneider J, Iori G, Ramiandrisoa D, Hammami M, Gräsel M, Chappard C, Barkmann R, Laugier P, Grimal Q, Minonzio J-G, et al. Ex vivo cortical porosity and thickness predictions at the tibia using full-spectrum ultrasonic guided-wave analysis. Archives of osteoporosis 2019;14(1):1–11.

[76] Shiraishi K, Chiba K, Okazaki N, Yokota K, Nakazoe Y, Kidera K, Yonekura A, Tomita M, Osaki M. In vivo analysis of subchondral trabecular bone in patients with osteoarthritis of the knee using second-generation high-resolution peripheral quantitative computed tomography (HR-pQCT). Bone 2020;132:115155.

[77] Boutroy S, Bouxsein ML, Munoz F, Delmas PD. In vivo assessment of trabecular bone microarchitecture by high-resolution peripheral quantitative computed tomography. The Journal of Clinical Endocrinology & Metabolism 2005;90(12):6508–15.

[78] Jiang H, Robinson DL, McDonald M, Lee PVS, Kontulainen SA, Johnston JD, Yates CJ, Wark JD. Predicting experimentally-derived failure load at the distal radius using finite element modelling based on peripheral quantitative computed tomography cross-sections (pQCT-FE): A validation study. Bone 2019;129:115051.

[79] Jiang H, Robinson DL, Yates CJ, Lee P, Wark JD. Peripheral quantitative computed tomography (pQCT)–based finite element analysis provides enhanced diagnostic performance in identifying non-vertebral fracture patients compared with dual-energy x-ray absorptiometry. Osteoporosis International 2020;31(1):141–51.

[80] Arpitha A, Rangarajan L. Computational techniques to segment and classify lumbar compression fractures. La radiologia medica 2020;125(6):551–60.

[81] Maciel JG, Araújo IMd, Trazzi LC, Azevedo-Marques PMd, Salmon CEG, Paula FJAd, Nogueira-Barbosa MH. Association of bone mineral density with bone texture attributes extracted using routine magnetic resonance imaging. Clinics 2020;75.

[82] Chang G, Boone S, Martel D, Rajapakse CS, Hallyburton RS, Valko M, Honig S, Regatte RR. Mri assessment of bone structure and microarchitecture. Journal of Magnetic Resonance Imaging 2017;46(2):323–37.

[83] Chang G, Honig S, Liu Y, Chen C, Chu KK, Rajapakse CS, Egol K, Xia D, Saha PK, Regatte RR. 7 tesla MRI of bone microarchitecture discriminates between women without and with fragility fractures who do not differ by bone mineral density. Journal of bone and mineral metabolism 2015;33(3):285–93.

[84] Wu H-Z, Zhang X-F, Han S-M, Cao L, Wen J-X, Wu W-J, Gao B-L. Correlation of bone mineral density with MRI t2* values in quantitative analysis of lumbar osteoporosis. Archives of osteoporosis 2020;15(1):1–7.

[85] Tognarelli JM, Dawood M, Shariff MIF, Grover VPB, Crossey MME, Cox IJ, Taylor-Robinson SD, McPhail MJW. Magnetic resonance spectroscopy: principles and techniques: lessons for clinicians. Journal of clinical and experimental hepatology 2015;5(4):320–8.

[86] Karampinos DC, Ruschke S, Dieckmeyer M, Diefenbach M, Franz D, Gersing AS, Krug R, Baum T. Quantitative MRI and spectroscopy of bone marrow. Journal of Magnetic Resonance Imaging 2018;47(2):332–53.

[87] Njeh CF, Hans D, Li J, Fan B, Fuerst T, He YQ, Tsuda-Futami E, Lu Y, Wu CY, Genant HK. Comparison of six calcaneal quantitative ultrasound devices: precision and hip fracture discrimination. Osteoporosis International 2000;11(12):1051–62.

[88] Krieg M-A, Barkmann R, Gonnelli S, Stewart A, Bauer DC, Barquero LDR, Kaufman JJ, Lorenc R, Miller PD, Olszynski WP, et al. Quantitative ultrasound in the management of osteoporosis: the 2007 ISCD official positions. Journal of Clinical Densitometry 2008;11(1):163–87.

[89] Bala Y, Zebaze R, Ghasem-Zadeh A, Atkinson EJ, Iuliano S, Peterson JM, Amin S, Bjørnerem A, Melton III LJ, Johansson H, et al. Cortical porosity identifies women with osteopenia at increased risk for forearm fractures. Journal of Bone and Mineral Research 2014;29(6):1356–62.

[90] Karjalainen JP, Riekkinen O, Töyräs J, Jurvelin JS, Kröger H. New method for point-of-care osteoporosis screening and diagnostics. Osteoporosis International 2016;27(3):971–7.

[91] Karjalainen JP, Riekkinen O, Kröger H. Pulse-echo ultrasound method for detection of post-menopausal women with osteoporotic BMD. Osteoporosis International 2018;29(5):1193–9.

[92] Prevrhal S, Engelke K, Kalender WA. Accuracy limits for the determination of cortical width and density: the influence of object size and CT imaging parameters. Physics in Medicine & Biology 1999;44(3):751.

[93] Ta D, Wang W, Wang Y, Le LH, Zhou Y. Measurement of the dispersion and attenuation of cylindrical ultrasonic guided waves in long bone. Ultrasound in medicine & biology 2009;35(4):641–52.

[94] Lefebvre F, Deblock Y, Campistron P, Ahite D, Fabre JJ. Development of a new ultrasonic technique for bone and biomaterials in vitro characterization. Journal of Biomedical Materials Research: An Official Journal of The Society for Biomaterials, The Japanese Society for Biomaterials, and The Australian Society for Biomaterials and the Korean Society for Biomaterials 2002;63(4):441–6.

[95] Minonzio J-G, Foiret J, Moilanen P, Pirhonen J, Zhao Z, Talmant M, Timonen J, Laugier P. A free plate model can predict guided modes propagating in tubular bone-mimicking phantoms. The Journal of the Acoustical Society of America 2015;137(1):EL98–104.

[96] Pereira D, Fernandes J, Belanger P. Ex-vivo assessment of cortical bone properties using low-frequency ultrasonic guided waves. IEEE Transactions on Ultrasonics, Ferroelectrics, and Frequency Control 2019;67(5):910–22.

[97] Schneider J, Ramiandrisoa D, Armbrecht G, Ritter Z, Felsenberg D, Raum K, Minonzio J-G. In vivo measurements of cortical thickness and porosity at the proximal third of the tibia using guided waves: Comparison with site-matched peripheral quantitative computed tomography and distal high-resolution peripheral quantitative computed tomography. Ultrasound in medicine & biology 2019;45(5):1234–42.

[98] Chiba K, Suetoshi R, Cretin D, Arai T, Kawajiri T, Okayama A, Tsuji S, Okazaki N, Osaki M, Yoh K. Development of a QUS device to evaluate deterioration of cortical bone: Verification by HR-pQCT and measurements in healthy individuals and dialysis patients. Journal of Clinical Densitometry 2020.

[99] Olszynski WP, Davison KS, Adachi JD, Brown JP, Hanley DA. Change in quantitative ultrasound-assessed speed of sound as a function of age in women and men and association with the use of antiresorptive agents: The canadian multicentre osteoporosis study. Journal of Clinical Densitometry 2019.

[100] Ishimoto T, Suetoshi R, Cretin D, Hagihara K, Hashimoto J, Kobayashi A, Nakano T. Quantitative ultrasound (QUS) axial transmission method reflects anisotropy in micro-arrangement of apatite crystallites in human long bones: A study with 3-MHz-frequency ultrasound. Bone 2019;127:82–90.

[101] Ghavami S, Denis M, Gregory A, Webb J, Bayat M, Kumar V, Fatemi M, Alizad A. Pulsed vibro-acoustic method for assessment of osteoporosis & osteopenia: A feasibility study on human subjects. Journal of the mechanical behavior of biomedical materials 2019;97:187–97.

[102] Dragomiretskiy K, Zosso D. Variational mode decomposition. IEEE transactions on signal processing 2013;62(3):531–44.

[103] Barkmann R, Rohrschneider W, Vierling M, Tröger J, De Terlizzi F, Cadossi R, Heller M, Glüer C-C. German pediatric reference data for quantitative transverse transmission ultrasound of finger phalanges. Osteoporosis International 2002;13 (1):55–61.

[104] Hartl F, Tyndall A, Kraenzlin M, Bachmeier C, Gückel C, Senn U, Hans D, Theiler R. Discriminatory ability of quantitative ultrasound parameters and bone mineral density in a population-based sample of postmenopausal women with vertebral fractures: Results of the basel osteoporosis study. Journal of Bone and Mineral Research 2002;17(2):321–30.

[105] de Moraes AM, Carvalho HM, Gonçalves EM, Guerra-Júnior G. Quantitative ultrasonography measurements of the phalanges in adolescents: A mixed longitudinal study. Ultrasound in Medicine & Biology 2017;43(12):2934–8.

[106] McCloskey EV, Kanis JA, Oden A, Harvey NC, Bauer D, González-Macias J, Hans D, Kaptoge S, Krieg MA, Kwok T, et al. Predictive ability of heel quantitative ultrasound for incident fractures: an individual-level meta-analysis. Osteoporosis International 2015;26(7):1979–87.

[107] Langton CM, Njeh CF. The measurement of broadband ultrasonic attenuation in cancellous bone-a review of the science and technology. ieee transactions on ultrasonics, ferroelectrics, and frequency control 2008;55(7):1546–54.

[108] Wear KA. Mechanisms of interaction of ultrasound with cancellous bone: A review. IEEE transactions on ultrasonics, ferroelectrics, and frequency control 2019;67(3):454–82.

[109] Aygun H. A review of the state of art in applying biot theory to acoustic propagation through the bone. A Review of the State of Art in Applying Biot 2014; 1:994–1008.

[110] Hosokawa A, Otani T. Ultrasonic wave propagation in bovine cancellous bone. The Journal of the Acoustical Society of America 1997;101(1):558–62.

[111] Otani T. Quantitative estimation of bone density and bone quality using acoustic parameters of cancellous bone for fast and slow waves. Japanese journal of applied physics 2005;44(6S):4578.

[112] Sai H, Iguchi G, Tobimatsu T, Takahashi K, Otani T, Horii K, Mano I, Nagai I, Iio H, Fujita T, et al. Novel ultrasonic bone densitometry based on two longitudinal waves: significant correlation with pQCT measurement values and age-related changes in trabecular bone density, cortical thickness, and elastic modulus of trabecular bone in a normal japanese population. Osteoporosis international 2010;21(10):1781–90.

[113] Li Y, Li B, Xu F, Liu C, Ta D, Wang W. Ultrasonic backscatter measurements at the calcaneus: An in vivo study. Measurement 2018;122:128–34.

[114] Liu C, Xu F, Ta D, Tang T, Jiang Y, Dong J, Wang W-P, Liu X, Wang Y, Wang W-Q. Measurement of the human calcaneus in vivo using ultrasonic backscatter spectral centroid shift. Journal of Ultrasound in Medicine 2016;35(10):2197–208.

[115] Li Y, Li B, Li Y, Liu C, Xu F, Zhang R, Ta D, Wang W. The ability of ultrasonic backscatter parametric imaging to characterize bovine trabecular bone. Ultrasonic imaging 2019;41(5):271–89.

[116] Conversano F, Franchini R, Greco A, Soloperto G, Chiriacò F, Casciaro E, Aventaggiato M, Renna MD, Pisani P, Di Paola M, et al. A novel ultrasound methodology for estimating spine mineral density. Ultrasound in medicine & biology 2015;41(1):281–300.

[117] Di Paola M, Gatti D, Viapiana O, Cianferotti L, Cavalli L, Caffarelli C, Conversano F, Quarta E, Pisani P, Girasole G, et al. Radiofrequency echographic multispectrometry compared with dual x-ray absorptiometry for osteoporosis diagnosis on lumbar spine and femoral neck. Osteoporosis International 2019;30 (2):391–402.

[118] Adami G, Arioli G, Bianchi G, Brandi ML, Caffarelli C, Cianferotti L, Gatti D, Girasole G, Gonnelli S, Manfredini M, et al. Radiofrequency echographic multi spectrometry for the prediction of incident fragility fractures: A 5-year follow-up study. Bone 2020;134:115297.

[119] Diez-Perez A, Brandi ML, Al-Daghri N, Branco JC, Bruyère O, Cavalli L, Cooper C, Cortet B, Dawson-Hughes B, Dimai HP, et al. Radiofrequency echographic multi-spectrometry for the in-vivo assessment of bone strength: state of the art-outcomes of an expert consensus meeting organized by the european society for clinical and economic aspects of osteoporosis, osteoarthritis and musculoskeletal diseases (ESCEO). Aging clinical and experimental research 2019:1–15.

[120] Kanis JA, Johnell O, Odén A, Johansson H, McCloskey E. Frax and the assessment of fracture probability in men and women from the uk. Osteoporosis international 2008;19(4):385–97.

[121] Kanis JA, Harvey NC, Johansson H, Liu E, Vandenput L, Lorentzon M, Leslie WD, McCloskey EV. A decade of FRAX: how has it changed the management of osteoporosis? Aging Clinical and Experimental Research 2020:1–10.

[122] Kanis JA, Cooper C, Rizzoli R, Reginster J-Y, et al. European guidance for the diagnosis and management of osteoporosis in postmenopausal women. Osteoporosis International 2019;30(1):3–44.

[123] Kanis JA, McCloskey EV, Johansson H, Oden A, Ström O, Borgström F. Development and use of FRAX® in osteoporosis. Osteoporosis international 2010; 21(2):407–13.

[124] Kanis JA, Harvey NC, McCloskey E, Bruyère O, Veronese N, Lorentzon M, Cooper C, Rizzoli R, Adib G, Al-Daghri N, et al. Algorithm for the management of patients at low, high and very high risk of osteoporotic fractures. Osteoporosis International 2020;31(1):1–12.

[125] Kanis JA, Harvey NC, Johansson H, Odén A, Leslie WD, McCloskey EV. Frax update. Journal of Clinical Densitometry 2017;20(3):360–7.

[126] Giangregorio LM, Leslie WD. Time since prior fracture is a risk modifier for 10-year osteoporotic fractures. Journal of Bone and Mineral Research 2010;25(6): 1400–5.

[127] Balasubramanian A, Zhang J, Chen L, Wenkert D, Daigle SG, Grauer A, Curtis JR. Risk of subsequent fracture after prior fracture among older women. Osteoporosis International 2019;30(1):79–92.

[128] Edwards BJ. Osteoporosis risk calculators. Journal of Clinical Densitometry 2017; 20(3):379–88.

[129] Beaudoin C, Moore L, Gagné M, Bessette L, Ste-Marie LG, Brown JP, Jean S. Performance of predictive tools to identify individuals at risk of non-traumatic fracture: a systematic review, meta-analysis, and meta-regression. Osteoporosis International 2019;30(4):721–40.

[130] Kanis JA, Harvey NC, Johansson H, Odén A, McCloskey EV, Leslie WD. Overview of fracture prediction tools. Journal of Clinical Densitometry 2017;20(3):444–50.

[131] Billington EO, Gamble GD, Reid IR. Reasons for discrepancies in hip fracture risk estimates using FRAX and garvan calculators. Maturitas 2016;85:11–8.

[132] Liang C, Sun FP, Rogers CA. Coupled electro-mechanical analysis of adaptive material systems-determination of the actuator power consumption and system energy transfer. Journal of Intelligent Material Systems and Structures 1994;5(1): 12–20.

[133] Lopes Jr V, Park G, Cudney HH, Inman DJ. Impedance-based structural health monitoring with artificial neural networks. Journal of Intelligent Material Systems and Structures 2000;11(3):206–14.

[134] Cortez NE, Filho JV, Baptista FG. A new microcontrolled structural health monitoring system based on the electromechanical impedance principle. Structural Health Monitoring 2013;12(1):14–22.

[135] Cortez NE, Filho JV, Baptista FG. Design and implementation of wireless sensor networks for impedance-based structural health monitoring using zigbee and global system for mobile communications. Journal of Intelligent Material Systems and Structures 2015;26(10):1207–18.

[136] de Castro BA, Baptista FGa, Ciampa F. A comparison of signal processing techniques for impedance-based damage characterization in carbon fibers under noisy inspections. Materials Today: Proceedings 2020.

[137] Srivastava S, Bhalla S, Madan A. Assessment of human bones encompassing physiological decay and damage using piezo sensors in non-bonded configuration. Journal of intelligent material systems and structures 2017;28(14):1977–92.

[138] Bhalla S, Bajaj S. Bone characterization using piezotransducers as biomedical sensors. Strain 2008;44(6):475–8.

[139] Bhalla S, Suresh R. Condition monitoring of bones using piezo-transducers. Meccanica 2013;48(9):2233–44.

[140] Mazlina MH, Bibi SSN, Tawie R, Daho CD, Annuar I. Bone-crack detection by piezoeletric-electromechanical impedance method. 2015 International Conference on Computer, Communications, and Control Technology (I4CT). IEEE; 2015. p. 418–21.

[141] Srivastava S, Bhalla S, Madan A. Shape memory alloy actuation of non-bonded piezo sensor configuration for bone diagnosis and impedance based analysis. Biomedical Engineering Letters 2019;9(4):435–47.

[142] Srivastava S, Bhalla S. Numerical evaluation of nonbonded piezo sensor for biomedical diagnostics using electromechanical impedance technique. International journal for numerical methods in biomedical engineering 2019;35 (2):e3160.

[143] Prakash S, Srivastava S, Bhalla S. Evaluation of bone electro-mechano gram (EMG) as a low-cost substitution of DEXA for osteoporosis detection. Health Monitoring of Structural and Biological Systems IX. vol. 11381. International Society for Optics and Photonics; 2020. p. 113812Q.

[144] Jurist JM. In vivo determination of the elastic response of bone. i. method of ulnar resonant frequency determination. Physics in Medicine & Biology 1970;15(3): 417.

[145] Bediz B, Özgüven HN, Korkusuz F. Vibration measurements predict the mechanical properties of human tibia. Clinical biomechanics 2010;25(4):365–71.

[146] Razaghi H, Saatchi R, Offiah AC. Neural network analysis of bone vibration signals to assesses bone density. Advances in Asset Management and Condition Monitoring. Springer; 2020. p. 1285–95.

[147] Razaghi H, Saatchi R, Bishop NJ, Burke D, Offiah H. Evaluation of vibration analysis to assess bone mineral density in children. WSEAS Transactions on Biology and Biomedicine 2020;17:39–47.

[148] Scanlan J, Li FF, Umnova O, Rakoczy G, Lövey N, Scanlan P. Detection of osteoporosis from percussion responses using an electronic stethoscope and machine learning. Bioengineering 2018;5(4):107.

[149] Hassan SS, Al Juboori AM. Evaluation the sensitivity of bone natural frequency as a diagnosis tool to identify bones integrity. MS&E 2020;765(1):012055.

[150] Meaney PM, Goodwin D, Golnabi AH, Zhou T, Pallone M, Geimer SD, Burke G, Paulsen KD. Clinical microwave tomographic imaging of the calcaneus: A first-in-human case study of two subjects. IEEE transactions on biomedical engineering 2012;59(12):3304–13.

[151] Amin B, Shahzad A, Farina L, Parle E, McNamara L, O'Halloran M, Elahi MA. Dielectric characterization of diseased human trabecular bones at microwave frequency. Medical engineering & physics 2020;78:21–8.

[152] Makarov SN, Noetscher GM, Arum S, Rabiner R, Nazarian A. concept of a radiofrequency device for osteopenia/osteoporosis screening. Scientific reports 2020;10(1):1–15.

[153] Watt J, Borhani R, Katsaggelos A. Machine learning refined: foundations, algorithms, and applications. Cambridge University Press; 2020.

[154] Bishop CM. Pattern recognition and machine learning. springer; 2006.

[155] Erjiang E, Wang T, Yang L, Dempsey M, Brennan A, Yu M, Chan WP, Whelan B, Silke C, O'Sullivan M, et al. Machine learning can improve clinical detection of low BMD: the DXA-HIP study. Journal of Clinical Densitometry 2020.

[156] Shim J-G, Kim DW, Ryu K-H, Cho E-A, Ahn J-H, Kim J-I, Lee SH. Application of machine learning approaches for osteoporosis risk prediction in postmenopausal women. Archives of Osteoporosis 2020;15(1):1–9.

[157] Ferizi U, Honig S, Chang G. Artificial intelligence, osteoporosis and fragility fractures. Current opinion in rheumatology 2019;31(4):368.

[158] Smets J, Shevroja E, Hügle T, Leslie WD, Hans D. Machine learning solutions for osteoporosisa review. Journal of Bone and Mineral Research 2021.

[159] Wani IM, Arora S. Computer-aided diagnosis systems for osteoporosis detection: A comprehensive survey. Medical & Biological Engineering & Computing 2020: 1–45.

[160] Martineau P, Leslie WD. The utility and limitations of using trabecular bone score with FRAX. Current opinion in rheumatology 2018;30(4):412–9.

[161] Viswanathan M, Reddy S, Berkman N, Cullen K, Middleton JC, Nicholson WK, Kahwati LC. Screening to prevent osteoporotic fractures: updated evidence report and systematic review for the US preventive services task force. Jama 2018;319 (24):2532–51.